View metadata, citation and similar papers at core.ac.uk

brought to you by CORE

provided by Open Research Online

Open Research Online

The Open University's repository of research publications
and other research outputs

Ground-based monitoring of comet 67P/Churyumov-Gerasimenko gas activity throughout the *Rosetta* mission

Journal Item

How to cite:

Opitom, C.; Snodgrass, C.; Fitzsimmons, A.; Jehin, E.; Manfroid, J.; Tozzi, G. P.; Faggi, S. and Gillon, M. (2017). Ground-based monitoring of comet 67P/Churyumov-Gerasimenko gas activity throughout the Rosetta mission. Monthly Notices of the Royal Astronomical Society, 469(S2) S222-S229.

For guidance on citations see FAQs.

© 2017 The Authors

Version: Version of Record

Link(s) to article on publisher's website:
http://dx.doi.org/doi:10.1093/mnras/stx1591

Copyright and Moral Rights for the articles on this site are retained by the individual authors and/or other copyright owners. For more information on Open Research Online's data policy on reuse of materials please consult the policies page.

oro.open.ac.uk

Monthly Notices
of the
ROYAL ASTRONOMICAL SOCIETY

MNRAS **469,** S222–S229 (2017)
Advance Access publication 2017 July 13

doi:10.1093/mnras/stx1591

Ground-based monitoring of comet 67P/Churyumov–Gerasimenko gas activity throughout the *Rosetta* mission

C. Opitom,[1⋆] C. Snodgrass,[2] A. Fitzsimmons,[3] E. Jehin,[4] J. Manfroid,[4] G. P. Tozzi,[5] S. Faggi[5] and M. Gillon[4]

[1]*European Southern Observatory, Avda. Alonso de Cordova 3107 Vitacura, Casilla 19001, Santiago de Chile, Chile*
[2]*School of Physical Sciences, The Open University, Milton Keynes, MK7 6AA, UK*
[3]*Astrophysics Research Centre, School of Mathematics and Physics, Queen's University Belfast, Belfast BT7 1NN, UK*
[4]*Space Sciences, Technologies and Astrophysics Research (STAR) Institute, Université de Liège, allée du 6 Août 17, B-4000 Liège, Belgium*
[5]*INAF, Osservatorio Astrofisico di Arcetri, Largo E. Fermi 5, I-50 125 Firenze, Italy*

Accepted 2017 June 21. Received 2017 June 13; in original form 2017 April 7

ABSTRACT

Simultaneously to the ESA *Rosetta* mission, a world-wide ground-based campaign provided measurements of the large scale activity of comet 67P/Churyumov–Gerasimenko through measurement of optically active gas species and imaging of the overall dust coma. We present more than 2 yr of observations performed with the FORS2 low-resolution spectrograph at the VLT, TRAPPIST and ACAM at the WHT. We focus on the evolution of the CN production as a tracer of the comet activity. We find that it is asymmetric with respect to perihelion and different from that of the dust. The CN emission is detected for the first time at 1.34 au pre-perihelion and production rates then increase steeply to peak about 2 weeks after perihelion at $(1.00 \pm 0.10) \times 10^{25}$ molecules s^{-1}, while the post-perihelion decrease is more shallow. The evolution of the comet activity is strongly influenced by seasonal effects with enhanced CN production when the Southern hemisphere is illuminated.

Key words: comets: individual: 67P/Churyumov–Gerasimenko.

1 INTRODUCTION

On 2016 September 30 the ESA *Rosetta* mission came to an end, after more than 2 yr of studying comet 67P/Churyumov–Gerasimenko (hereafter 67P). A variety of instruments onboard *Rosetta* and the lander *Philae* allowed to study with unprecedented details both the nucleus and the coma of 67P, and to monitor its evolution over more than 2 yr while the comet was approaching the Sun, and after its perihelion passage.

Simultaneously to the mission, a ground-based campaign[1] was set up, involving a large number of telescopes all over the world observing at various wavelengths (Snodgrass et al. 2017). The main goals of that campaign were to assess the total activity of the comet by observing the coma at scales larger than those probed by the spacecraft and to place the observations of other comets in context by comparing ground-based and *in situ* observations of 67P. We present here more than 2 yr of low-resolution spectroscopic observations of 67P performed with the FORS2 instrument at the VLT along with observations performed with the 60cm TRAPPIST at La Silla and the William Herschel Telescope (WHT) on La Palma. Combining those observations, we study the evolution of 67P gas activity over a large part of the comet orbit, simultaneously to the *in situ* measurements performed with *Rosetta* and *Philae*.

2 OBSERVATIONS AND DATA REDUCTION

In this section, we present the observations performed with VLT/FORS2, TRAPPIST and WHT/ACAM, along with the data reduction procedure. The observing geometry of the comet during this apparition was not favourable for ground-based observers, especially from the Southern hemisphere. Around the time of perihelion, the comet was low on the horizon and difficult to observe. Because of this, the number of gas species that could be detected from the ground is limited and most of them could only be detected around the time of perihelion. The only species that could be detected over a wide range of heliocentric distances is CN. This work thus focuses mainly on the evolution of comet 67P's CN production rate.

2.1 VLT/FORS2

Spectra of comet 67P were obtained with the FORS2 instrument at the VLT (Appenzeller et al. 1998) in Long-slit spectroscopy (LSS) mode, over a period of more than 2 yr. The FORS2 is equipped with a mosaic of two 2k × 4k MIT CCDs, providing a spatial

⋆ E-mail: copitom@eso.org
[1] http://www.rosetta-campaign.net

© 2017 The Authors
Published by Oxford University Press on behalf of the Royal Astronomical Society

Table 1. VLT/FORS2 observational circumstances and derived gas production rates.

Date	r (au)	$\dot{r}$ (km s^{-1})	Δ (au)	Setup	t_{exp} (s)	N_{exp}	Q(CN) (mol s^{-1})
2014-May-6	4.08	− 8.40	3.60	FORS 150I	600	6	<3.2E24
2014-June-4	3.93	− 8.80	3.10	FORS 150I	600	6	<1.9E24
2014-June-24	3.83	− 9.15	2.85	FORS 150I	600	25	<1.0E24
2014-July-20–21	3.69	− 9.60	2.70	FORS 300V	900	25	<6.4E23
2014-August-15–16	3.54	− 10.00	2.74	FORS 300V	900	11	<6.7E23
2014-September-23	3.31	− 10.70	3.02	FORS 300V	900	4	<1.1E24
2014-October-18–25	3.13	− 11.26	3.27	FORS 300V	600, 900	16	<4.3E23
2014-November-15–23	2.94	− 11.74	3.45	FORS 300V	700, 750, 800, 900	14	<4.6E23
2015-May-22	1.59	− 11.94	2.25	FORS 300V	300	3	<7.6E23
2015-July-2	1.34	− 7.70	1.90	FORS 300V	300	3	1.34 ± 0.80E24
2015-July-8	1.32	− 6.93	1.87	FORS 600B	600	1	2.39 ± 0.50E24
2015-November-12	1.66	12.40	1.79	FORS 600B	300	1	3.61 ± 0.80E24
2015-December-1	1.79	13.03	1.75	FORS 600B	300	3	2.27 ± 0.21E24
2015-December-12	1.87	13.23	1.71	FORS 600B	300	3	1.94 ± 0.16E24
2015-December-20	1.93	13.31	1.68	FORS 600B+300V	300	3	2.09 ± 0.25E24
2015-December-22	1.95	13.33	1.67	FORS 600B	300	3	1.96 ± 0.18E24
2016-January-12	2.11	13.35	1.57	FORS 600B+300V	300	7	1.82 ± 0.18E24
2016-February-4	2.28	13.18	1.50	FORS 600B	300	3	1.01 ± 0.12E24
2016-February-14	2.36	13.07	1.48	FORS 600B+300V	600	6	1.42 ± 0.25E24
2016-March-4	2.50	12.80	1.53	FORS 600B	600	3	1.27 ± 0.15E24
2016-March-14	2.57	12.65	1.59	FORS 600B	600	3	1.05 ± 0.11E24
2016-March-28	2.67	12.42	1.72	FORS 600B	600	3	1.17 ± 0.16E24
2016-March-30	2.69	12.38	1.75	FORS 600B	600	2	5.58 ± 1.49E23
2016-April-7	2.75	12.25	1.85	FORS 600B	600	2	6.92 ± 3.97E23
2016-April-10	2.77	12.20	1.89	FORS 300V	600	3	6.39 ± 1.75E23
2016-April-30	2.91	11.84	2.22	FORS 600B	900	3	9.03 ± 2.03E23
2016-May-30	3.11	11.28	2.82	FORS 600B	300	6	<7.20E23
2016-June-20	3.25	10.89	3.26	FORS 600B	1200	3	–
2017-January-30	4.41	7.30	4.34	FORS 600B	1200	3	–
2017-March-3	4.54	6.86	3.97	FORS 600B	1200	3	–

Notes. r *is the heliocentric distance of the comet;* $\dot{r}$ *the heliocentric velocity;* Δ *the geocentric distance; and* $\dot{\Delta}$ *the geocentric velocity.* t_{exp} *and* N_{exp} *are respectively the exposure time (in seconds) and the number of exposures used to compute the gas production rate.*

resolution of 0.25 arcsec pix^{-1} with the standard collimator and the 2 × 2 binned readout mode. FORS2 slit is 6.8 arcmin long and we used a 1.3 arcsec-wide slit. For all observations, the slit was aligned with the parallactic angle. The goal of the observations performed in 2014 was mainly to monitor the dust activity of the comet and measure the slope of the continuum (Snodgrass et al. 2016b). From observations of comet 67P during previous perihelion passages, it was reported that the activity of the comet is lower inbound than outbound (Schleicher 2006), and we were not expecting to detect gas at large heliocentric distances pre-perihelion. We used the 150I grism, providing a wide wavelength coverage from 330 to 1100 nm (central wavelength $\lambda_c = 720$ nm) with very low resolution ($R = 260$). As the comet got closer to the Sun, we started to use also the 300V grism, which has a bluer central wavelength and a higher resolution ($\lambda_c = 590$ nm, $R = 440$), to allow early detection of CN emission. In late 2014 and early 2015, the comet was not observable with the VLT, because of low solar elongation and high declination. It became visible again for a few weeks between late 2015 May and early July, shortly before the perihelion passage. At that time, it was low on the horizon and only visible for a short period each night. The best observations of comet 67P gas emissions with FORS2 were then performed after the perihelion passage, between 2015 November and 2016 June. For those observations (and for the last 2015 July observation), we also used the 600B grism, with a central wavelength of 465 nm and a spectral resolution of 780, to increase the signal-to-noise ratio of the emission bands. Finally, two more sets of spectra were obtained in early 2017, when the comet was at more than 4 au from the Sun. Solar analogues were observed regularly along the runs with the different grisms and were used to subtract the dust continuum.

The data reduction was done using a combination of the European Southern Observatory (ESO) pipeline and IRAF routines. Basic data reduction as well as wavelength and flux calibration were performed with the ESO/FORS2 pipeline to obtain 2D reduced spectra. The sky background was then determined from clean zones of the spectrum, and extrapolated to the whole spectrum using IRAF routines. Some spectra were discarded, either because star spectra were overlapping the comet, because of clouds, or simply because the comet was not visible in the spectrum. Table 1 lists the observations along with the observational circumstances and the instrumental setup (this Table only lists the spectra actually used for this work). We binned the 2D spectra by 10 pixels in the spatial direction to increase the signal-to-noise ratio and extracted each bin separately. Observations of solar analogues corrected from colour effects were used to subtract the continuum. Spatial profiles of CN were obtained by summing every extracted binned spectra over the 383–390.5 nm wavelength range. We obtained radial profiles on one side of the nucleus only since on the other side part of the extended CN emission was falling into the gap between the two FORS2 CCDs. Representative spectra for different epochs are illustrated in Fig. 1.

We converted the CN fluxes into column density using the fluorescence efficiencies from Schleicher (2010). Instead of using the

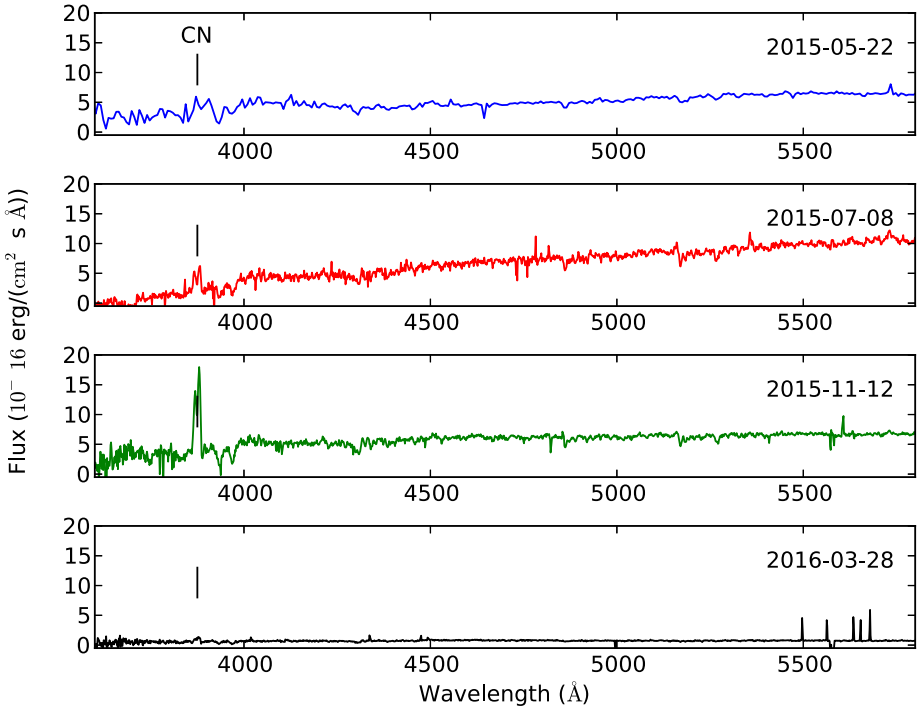

Figure 1. Examples of FORS2 sky-subtracted extracted spectra for four different dates: 2015 May 22, 2015 July 8, 2015 November 12 and 2016 March 28. Those spectra have been extracted out to 5 arcsec. The vertical line indicates the wavelength of the CN emission.

CN flux integrated in a given aperture to derive the CN production rate, we used the radial profile directly and adjusted a Haser model (Haser 1957) at a physical distance of about 10 000 km to compute CN production rates, similarly to what was done in Opitom et al. (2016). Deriving the production rate at a given physical distance in the coma instead of using a fixed aperture size allows us to avoid aperture effects, since the geocentric distance of the comet varies between 1.48 and more than 4 au during our observations. We used a constant outflow velocity of 1 km s^{-1} as assumed by A'Hearn et al. (1995), together with their scalelengths scaled as r^2, r being the heliocentric distance. The resulting gas production rates and upper limits are given in Table 1. For the last three observations, the comet was extremely faint and we could not derive constraining upper limits. The uncertainty of the gas production rates is estimated from the dispersion of measurements performed during the same night. When only one measurement is available, we estimate the uncertainty to be of 20 per cent (from the uncertainty on the background and dust subtraction).

2.2 TRAPPIST

Comet 67P was also observed with the TRAPPIST 60 cm robotic telescope (Jehin et al. 2011). TRAPPIST is equipped with a 2k × 2k FLI camera with a field of view of 22 arcmin × 22 arcmin. A set of narrow band filters designed for the observing campaign of comet Hale–Bopp is mounted on the filter wheel (Farnham, Schleicher & A'Hearn 2000), allowing us to isolate the emission of OH, NH, CN, C_3 and C_2, as well as several zones of the dust continuum free from gas emission. The filter wheel also contains a set of broad-band *B*, *V*, *Rc* and *Ic* Johnson–Cousin filters. We observed the comet once or twice a week between 2015 April 18 and 2016 June 7. Most observations were performed with broad-band filters, with exposure times ranging from 120 to 240 s. From those observations, we derived $Af\rho$ (A'Hearn et al. 1984) values and monitored the evolution of the dust activity, see for example Snodgrass et al. (2016a).

Around the time of perihelion, between 2015 August 22 and September 12, we were also able to detect CN and C_2 using narrow-band filters. The TRAPPIST data reduction procedure is described in detail in Opitom et al. (2015). Radial profiles were computed using an azimuthal median and then dust-subtracted. Similarly to what was done with the FORS2 observations, we used fluorescence efficiencies from Schleicher (2010) and A'Hearn et al. (1995) to compute CN and C_2 column densities respectively. The gas production rates were obtained by adjusting a Haser model at a physical distance around 10 000 km. The observational circumstances for the TRAPPIST observations are listed in Table 2 along with the measured production rates. The dispersion of the C_2 production rates is higher than for the CN because the signal in the C_2 filter was low and the dust contamination difficult to remove.

2.3 WHT/ACAM

Spectroscopy of comet 67P was attempted with the 4.2m William Herschel Telescope on the nights of 2015 July 7–8, 2015 July 27–28 and 2016 June 28–29. In all observations we used the ACAM instrument to obtain contextual SDSS *r*-band imaging and optical spectroscopy. ACAM is equipped with a 2k × 4k E2V chip and a low resolution 400 lines mm^{-1} VPH grating giving an uncontaminated first order spectrum covering ∼3300 − 6600 Å. Due to the bright and variable twilight sky background on these dates, only a 300 s exposure through a 2.0 arcsec width slit on July 28.21 UT allowed clear detection of the comet and CN emission. The comet was at $r = 1.26$ au and $\Delta = 1.80$ au. Data reduction and analysis used IRAF routines in a similar manner to the VLT observations, plus the IDL-based *procspec* package (Ryans 2017). The CN emission was extracted out to ±7.7 arcsec either side of the nucleus, equivalent to 10 000 km at the comet on this date. Using the same Haser

Table 2. TRAPPIST observational circumstances and derived gas production rates.

Date	r (au)	$\dot{r}$ (km s^{-1})	Δ (au)	Setup	t_{exp} (s)	N_{exp}	Q(CN) (mol s^{-1})	Q(C_2) (mol s^{-1})
2015-August-22	1.25	1.97	1.77	TRAPPIST	900	1	6.72 ± 0.64E24	–
2015-August-23	1.25	2.17	1.77	TRAPPIST	900	1	–	8.60 ± 0.74E24
2015-August-24	1.25	2.38	1.77	TRAPPIST	900	1	7.77 ± 0.82E24	–
2015-August-28	1.26	3.20	1.77	TRAPPIST	900	1	–	6.97 ± 1.32E24
2015-August-29	1.26	3.40	1.77	TRAPPIST	900	1	1.00 ± 0.10E25	–
2015-August-30	1.26	3.60	1.77	TRAPPIST	900	1	–	5.97 ± 0.97E24
2015-August-31	1.26	3.80	1.77	TRAPPIST	900	1	–	7.41 ± 1.67E24
2015-September-11	1.29	5.86	1.78	TRAPPIST	900	1	8.45 ± 0.93E24	–
2015-September-12	1.30	6.03	1.78	TRAPPIST	900	1	7.49 ± 0.90E24	–
2015-September-13	1.30	6.20	1.78	TRAPPIST	900	1	–	4.60 ± 1.13E24

Notes. r *is the heliocentric distance of the comet;* $\dot{r}$ *the heliocentric velocity;* Δ *the geocentric distance; and* $\dot{\Delta}$ *the geocentric velocity.* t_{exp} *and* N_{exp} *are respectively the exposure time (in seconds) and the number of exposures used to compute the gas production rate.*

model parameters as in Section 2.1, we obtained $Q(CN) = (3.15 \pm 0.36) \times 10^{24}$ molecules s^{-1} at this time.

3 EVOLUTION OF THE COMET ACTIVITY

In the following part of this work, we use FORS2, TRAPPIST and WHT/ACAM data altogether to study the evolution of comet 67P activity over a long time-scale since they cover different parts of the orbit. Even though the techniques are different, we use the same model along with the same model parameters to derive the CN production rates. We also compute gas production rates at a fixed physical distance in the coma to avoid introducing aperture trends in the data as the geocentric distance of the comet is changing. In addition, the consistency of TRAPPIST and VLT/FORS2 results has already been demonstrated using simultaneous observations of the same comet with the two instruments (Opitom et al. 2016).

Two years of VLT/FORS2 observations, combined with TRAPPIST and ACAM data, allow us to follow the evolution of comet 67P's gas activity over a large part of its orbit. The evolution of comet 67P's CN production rate as a function of the heliocentric distance is represented in Fig. 2. During the first part of the campaign, in 2014, when the comet was between 4 and 2.9 au from perihelion, no gas emission could be detected (Snodgrass et al. 2016b). This lack of gas detection at large distance from the Sun is consistent with upper limits measured at similar distances pre-perihelion during previous passages (Guilbert-Lepoutre et al. 2014).

When we recovered the comet on 2015 May 22 at 1.59 au from the Sun, we still could not clearly detect any gas emission, even though at this date we are probably close to the detection limit. Observations obtained on July 2 with the 300V grism allowed us to detect the CN emission for the first time, and observations obtained less than a week later with higher spectral resolution confirmed the detection. Starting around that time, it appears that the CN production rate increases very fast as the comet is approaching perihelion. We observe an increase of almost a factor of 2 between the last pre-perihelion FORS observation and the first TRAPPIST observation. The comet CN production rate peaks about 2 weeks after the perihelion passage at $(1.00 \pm 0.10) \times 10^{25}$ molecules s^{-1}. After the peak, the CN production decreases continuously as the comet moves away from the Sun, until the comet reaches 3 au, a distance at which we could not detect it anymore. Representative spectra of comet 67P obtained at different epochs shown in Fig. 1 illustrate the lack of clearly detected gas emission in 2015 May, and the sudden appearance of CN in early July. In 2015 November, the CN emission is clearly detected, while it is much fainter in late 2016 March.

In the upper part of Fig. 2, we overlay measurements (or upper limits) of the CN production rates performed during previous perihelion passages of the comet (Schulz et al. 2004; Schleicher 2006; Lara et al. 2011; Guilbert-Lepoutre et al. 2014). Both our measurements and upper limits are a good match to values reported for previous perihelion passages of the comet, indicating that the activity level of comet 67P does not decrease due to repeated passages close to the Sun. Similar to previous perihelion passages, the activity of the comet is very asymmetric with respect to perihelion. Prior to the perihelion passage, the upper limits we measure indicate that the CN production remains low as the comet approaches the Sun, up to until about 1.5 au; while after the perihelion passage, we detect CN up to 3 au. The increase of the CN production rate just before the perihelion passage is steeper than the activity decrease after the perihelion passage. Asymmetries of the activity about perihelion are not unusual for comets (A'Hearn et al. 1995; Schleicher, Millis & Birch 1998; Knight & Schleicher 2013), even though their origin is still poorly understood. Schleicher (2006) has already reported the asymmetry of comet 67P gas activity about perihelion and attributed it to a seasonal effect with a dominant active region starting to be illuminated around the time of perihelion.

A few other measurements of comet 67P CN production rate have been performed during this perihelion passage and are shown in the lower part of Fig. 2, amongst which those obtained with the LOTUS spectrograph at the Liverpool Telescope (Steele et al. 2016), reported in Snodgrass et al. (2016a). Almost simultaneous measurements performed on 2015 November 12 show a large discrepancy while production rates measured on December 10 with LOTUS agree within the error bars with the FORS2 value measured on December 12. The TRAPPIST and LOTUS measurements performed in September are consistent. The LOTUS measurements are also lower than those performed at similar heliocentric distances during previous apparitions of the comet. The origin of this discrepancy is still unclear. Similar models and model parameters have been used for our measurements and those reported by Schleicher (2006) and Snodgrass et al. (2016a) to derive CN production rates. However, we performed tests showing that aperture effects can be as strong as 30 or 40 per cent in this case. In addition, Schleicher (2006) report large short-term variability, probably due to the rotation of the nucleus. The nucleus of comet 67P has a rotation period of 12.4 h (Mottola et al. 2014) and important rotational variability was reported from *in situ* observations made by the ROSINA instrument onboard *Rosetta*, (see for example Hässig et al. 2015). We also

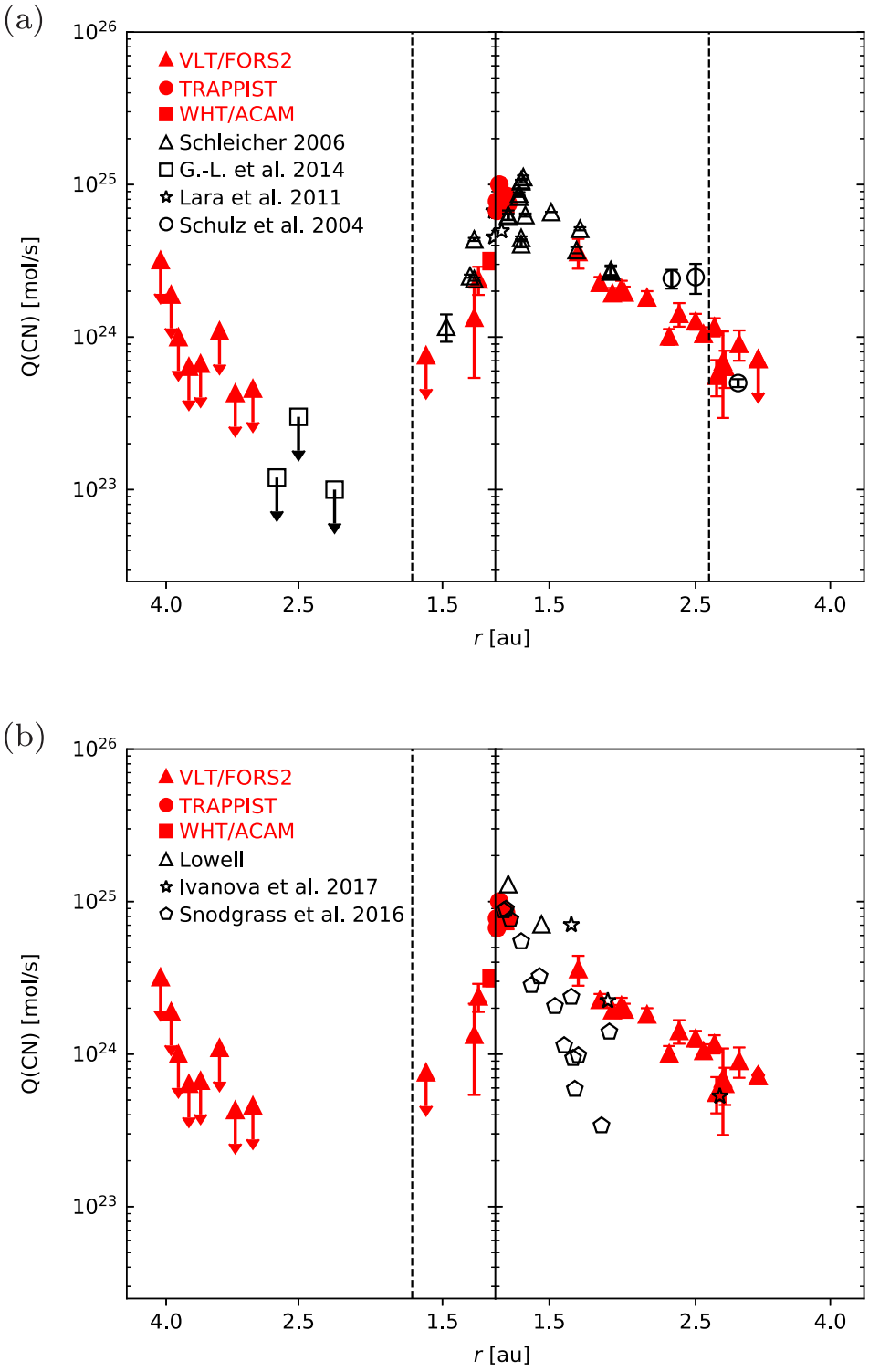

Figure 2. Pre- and post-perihelion evolution of comet 67P CN production rate. We include data obtained with VLT/FORS2 (red triangles), with TRAPPIST (red full circles) and with WHT/ACAM (red square). (a) We compare our results to measurements performed at previous perihelion passages (Schulz, Stüwe & Boehnhardt 2004; Schleicher 2006; Lara et al. 2011; Guilbert-Lepoutre et al. 2014). (b) We compare our results to measurements performed during this perihelion passage with the Liverpool Telescope (Snodgrass et al. 2016a), the SAO 6m (Ivanova et al. 2017) and the Lowell 1.1 m (Schleicher, personal communication). The two vertical dashed lines indicate the equinox.

point that there is an uncertainty in the automatic acquisition with the robotic Liverpool Telescope, which relies on the ephemeris of the object. As a consequence, the comet could be slightly off centre, which might explain the discrepancies we observe. Measurements performed with the Lowell 1.1 m telescope shortly after perihelion (Schleicher, personal communication), and others performed with the 6 m BTA telescope of the SAO (Ivanova et al. 2017) up to 3 au from the Sun, mostly agree with our measurements.

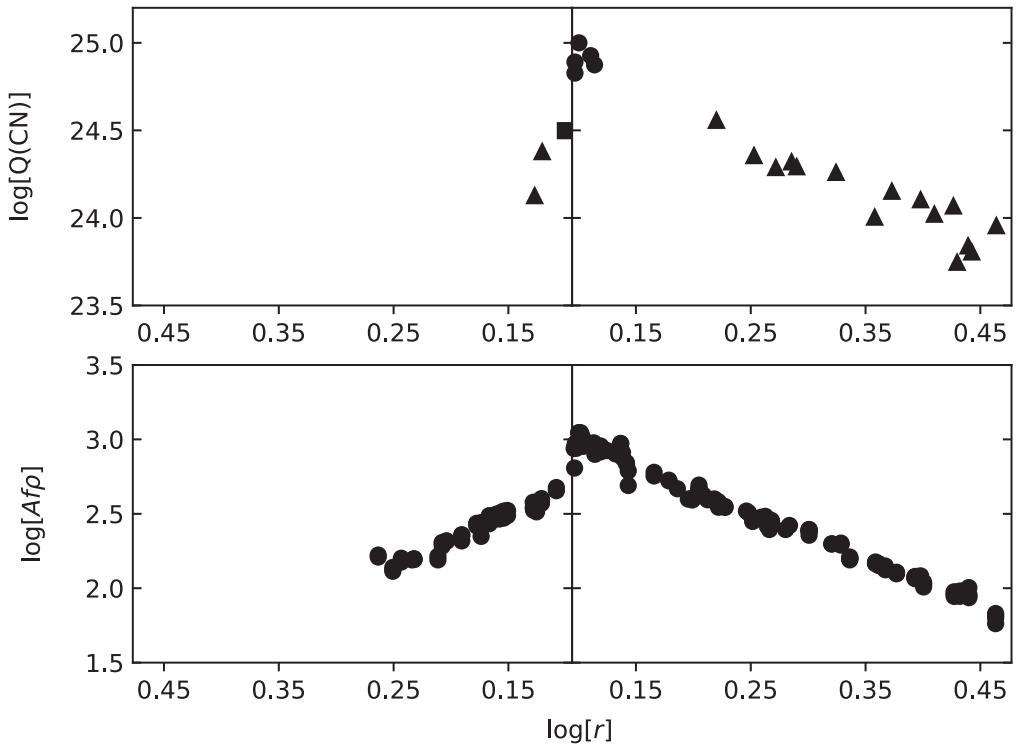

Figure 3. Evolution of 67P CN production rate (top) and $Af\rho$ (bottom) as a function of the heliocentric distance. Full circles represent measurements made from TRAPPIST observations, triangles represent measurements made from VLT/FORS2 observations and squares represent measurements made from WHT/ACAM observations. For clarity, we did not represent error bars.

In Fig. 3, we compare the evolution of the gas and dust activity of comet 67P. Similarly to the CN, the dust production peaks about 2 weeks after perihelion. However, the dust activity is not as asymmetric about perihelion as the gas. The absolute $Af\rho$ values measured post-perihelion are higher than those measured pre-perihelion at the same heliocentric distance but the power-law slopes of the $Af\rho$ variation with the heliocentric distance are similar on both sides of perihelion. We measured a power-law slope of -3.38 ± 0.13 pre-perihelion and a slope of -3.14 ± 0.04 post-perihelion, which is consistent with the predictions from Snodgrass et al. (2013) and simultaneous measurements made from Wendelstein observatory (Boehnhardt et al. 2016). In the case of CN, the number of detections pre-perihelion was insufficient to derive a reliable slope, but we derived a slope of -2.93 ± 0.15 for post-perihelion observations. The decrease of the CN production is similar to the decrease of the dust activity after the perihelion passage but the asymmetry about perihelion is stronger, as we were only able to detect the CN emission shortly before the perihelion passage.

We do no detect any outburst in our data, either around the time of perihelion or at larger distances. However, several outbursts were detected from the spacecraft instruments. Numerous small outbursts were detected around the time of perihelion (Vincent et al. 2016), and a more important one was also detected by several instruments on 2016 February 19 (Grün et al. 2016), for example. We do not see any evidence of increased dust or gas production at the time of the outbursts reported by Vincent et al. 2016 and Grün et al. 2016. One crucial difference between *in situ* and ground-based observations is the spatial scale we probe. From the ground, we observe a large part of the coma containing gas and dust emission from several nucleus rotations and short time-scale variations such as small outbursts are 'diluted'. In addition, the cadence of the ground-based observations presented here is typically two to three observations a week for the dust and even scarcer for the gas. A large part of small and short-lived cometary outbursts might then remain undetected from ground-based observations.

By computing the ratio between the C_2 and the CN production rates as measured with TRAPPIST, we can assess the chemical class of comet 67P. We do not have measurements of both production rates performed the same night, so we used mean values of the C_2 and CN production rates to compute a ratio of $Q(C_2)/Q(CN) = 0.83$. From this, 67P can be classified as a typical comet in terms of carbon chain species as defined by A'Hearn et al. (1995). The comet was classified as depleted by Cochran et al. (1992), Schulz et al. (2004) and Schleicher (2006), while it was classified as typical by Lara et al. (2011). This disparity can probably be explained by the fact that 67P is close to the limit between typical and depleted comets and has an important rotational variability, making the determination of the abundance ratio difficult without simultaneous measurements.

4 DISCUSSION

In this work, we used the CN production rate of 67P to estimate the general gas activity and production of the comet. From the ground, we were not able to monitor the production rate of water itself, or any of its dissociation product, over large time-scales. The OH radical was detected with the ISIS spectrograph at the WHT, but only around the time of perihelion. CN was the only gas species that could be monitored over a significant part of the orbit. However, we must be cautious while using CN as an indicator of the total gas activity of the comet, as the ratio between the water and CN production of a comet can vary both with time and the heliocentric distance. The CN production rate we measure might then not be

representative of the overall comet gas activity. In the case of 67P, Bockelée-Morvan et al. (2016) observed an increase by a factor of 2 of the ratio between highly volatile gases (CO_2, CH_4 and OCS) and water between 2015 July and September. The HCN abundance relative to water is then likely to vary too. Since the CN radical is thought to be produced by the photodissociation of HCN (Fray et al. 2005), the CN to water ratio might change at this epoch.

Measurements from various instruments onboard *Rosetta* indicate that the total gas activity of the comet was symmetrical about perihelion (Fougere et al. 2016; Hansen et al. 2016), while we observe an asymmetry of the CN production rate. Previous results from ground-based observations also indicate that the post-perihelion decrease of OH production rates is steeper than the decrease of CN production rates (Schleicher 2006). Studies of the evolution of production rates and of the activity distribution at the surface of the comet performed using the VIRTIS and ROSINA instruments onboard *Rosetta* (Bockelée-Morvan et al. 2016; Fougere et al. 2016) might help explain the evolution of CN production rate. They both suggest that the upper layers of the Northern hemisphere of the comet nucleus are depleted in highly volatiles species. Indeed, this hemisphere is illuminated over a long period of time (5.5 yr) during each orbit, when the comet moves away from the Sun following the previous perihelion passage and when it is approaching the Sun again. On the other hand, the Southern hemisphere is illuminated closer to the perihelion passage and then undergoes important out-gassing over a short period of time, constantly exposing new surface. Differences in the ratio of highly volatile gases to water are then expected to be observed between both hemispheres, and should cause changes of the coma gas composition, depending on the illuminated hemisphere.

Hoang et al. (2017) analyse more than a year of data obtained by the ROSINA instrument onboard *Rosetta*. They observe variations of the ratio between water, and CO and CO_2, depending on the illuminated hemisphere. Those variations are attributed to an icy dust layer covering the Northern hemisphere, which would have been deposited during the previous perihelion passage of the comet. This layer would prevent the heat to reach deeper layers rich in highly volatile gases. It is not clear whether the upper layers of the Northern hemisphere are depleted in highly volatile gases or if the layers rich in volatile species are buried under icy dust layers deposited during the previous perihelion. However, *in situ* measurements made with several instruments onboard *Rosetta* agree to indicate that the ratio between water and more volatile species varies with the season.

During the first part of our observations, from 2014 May to 2015 May, the Northern hemisphere was illuminated. At this time, we could not detect the CN emission in FORS2 spectra. Shortly after the first equinox, we detected the CN for the first time and the CN production started to increase steeply. After the comet perihelion passage, the CN production rate decreased at a slow pace until 2016 May, at which time we could not detect it anymore. The last CN detections are recorded shortly after the second equinox. The uppermost layers of the Northern hemisphere might be depleted in HCN, explaining why we were only able to detect CN after the first equinox, when the Southern hemisphere was illuminated. At that time, the production of CN increased steeply, reached a peak 2 weeks after perihelion and decreased slowly after.

We also observed differences between the evolution of the CN and dust activity measured from the ground. However, comparison between the water production rate measured by a variety of instruments onboard *Rosetta* (ROSINA, VIRTIS-H, VIRTIS-M, RPC-ICA, MIRO) and ground-based measurements showed surprisingly good agreement (Hansen et al. 2016). Once we account for the variation of the coma composition with the heliocentric distance, the evolution of the large-scale activity of 67P measured from ground-based observations is then generally in good agreement with *in situ* measurement from the *Rosetta* spacecraft.

The comparison of 67P activity as measured from the ground and *in situ* by *Rosetta* instruments is important to understand the evolution of comet activity in general. Here, we emphasized the importance of seasonal effects on the evolution of 67P activity and coma composition. Such changes have been reported for numerous other comets observed from the ground. The knowledge gathered from the synergy between *Rosetta* and ground-based observations will lead us to a better understanding of how the nucleus surface composition influences the comet activity and the coma composition and help us link future ground-based comet observations to what is actually happening in the nucleus.

5 CONCLUSIONS

This paper focused on the long-term monitoring of comet 67P/Churyumov–Gerasimenko gas activity performed with the VLT/FORS2 instrument, TRAPPIST, and WHT/ACAM. We find the following:

(i) The CN production rate of 67P is asymmetric with respect to perihelion. Our first CN detection occurs at only 1.34 au pre-perihelion. The CN production then increases steeply and peaks at $(1.00 \pm 0.10) \times 10^{25}$ molecules s^{-1} about 2 weeks after perihelion. Post-perihelion, the CN production rates decrease at a slower pace. The evolution of the CN production is different from that of the dust, which is more symmetrical about perihelion and is in good agreement with *in situ* water production measurements from the *Rosetta* mission.

(ii) Seasonal effects play an important role in the evolution of the comet activity. The illumination of the comet Southern hemisphere (shortly before and during the months after perihelion) corresponds to higher CN production rates. Differences in the upper layer composition of the two hemispheres, due to the conditions experienced during previous passages, have an impact on the evolution of the comet activity and coma composition.

(iii) The activity of the comet is consistent with what was observed at previous passages. We do not see a decrease of the activity due to repeated passages close to the Sun.

(iv) No outbursts are detected from our ground-based observations.

(v) Ground-based measurements of the comet activity are consistent with findings from *in situ* measurements made by *Rosetta* instruments.

ACKNOWLEDGEMENTS

This work is partly based on observations collected at the European Organization for Astronomical Research in the Southern hemisphere under ESO programmes 093.C–0593, 094.C–0054, 595.C–0066 and 097.C–0201. TRAPPIST–South is a project funded by the Belgian Fonds (National) de la Recherche Scientifique (F.R.S.–FNRS) under grant FRFC 2.5.594.09.F, with the participation of the Swiss National Science Foundation (FNS/SNSF). The William Herschel Telescope is operated on the island of La Palma by the Isaac Newton Group of Telescopes in the Spanish Observatorio del Roque de los Muchachos of the Instituto de Astrofísica de Canarias. EJ and MG are F.R.S.–FNRS research associates. AF was supported by UK STFC grant ST/L000709/1. CS was supported by a UK STFC Ernest Rutherford fellowship.

REFERENCES

A'Hearn M. F., Schleicher D. G., Millis R. L., Feldman P. D., Thompson D. T., 1984, AJ, 89, 579
A'Hearn M. F., Millis R. C., Schleicher D. O., Osip D. J., Birch P. V., 1995, Icarus, 118, 223
Appenzeller I. et al., 1998, The Messenger, 94, 1
Bockelée-Morvan D. et al., 2016, MNRAS, 462, S170
Boehnhardt H., Riffeser A., Kluge M., Ries C., Schmidt M., Hopp U., 2016, MNRAS, 462, S376
Cochran A. L., Barker E. S., Ramseyer T. F., Storrs A. D., 1992, Icarus, 98, 151
Farnham T., Schleicher D., A'Hearn M., 2000, Icarus, 147, 180
Fougere N. et al., 2016, MNRAS, 462, S156
Fray N., Bénilan Y., Cottin H., Gazeau M.-C., Crovisier J., 2005, Planet. Space Sci., 53, 1243
Grün E. et al., 2016, MNRAS, 462, S220
Guilbert-Lepoutre A., Schulz R., Rożek A., Lowry S. C., Tozzi G. P., Stüwe J. A., 2014, A&A, 567, L2
Hansen K. C. et al., 2016, MNRAS, 462, S491
Haser L., 1957, Bull. Acad. R. Sci. Belg., 63, 739
Hässig M. et al., 2015, Science, 347, aaa0276
Hoang M. et al., 2017, A&A, 600, A77
Ivanova O. et al., 2017, MNRAS, 469, 2695
Jehin E. et al., 2011, The Messenger, 145, 2
Knight M. M., Schleicher D. G., 2013, Icarus, 222, 691
Lara L. M., Lin Z.-Y., Rodrigo R., Ip W.-H., 2011, A&A, 525, A36
Mottola S. et al., 2014, A&A, 569, L2
Opitom C., Jehin E., Manfroid J., Hutsemékers D., Gillon M., Magain P., 2015, A&A, 574, A38
Opitom C. et al., 2016, A&A, 589, A8
Ryans R., 2017, https://star.pst.qub.ac.uk/rsir/procspec.html
Schleicher D. G., 2006, Icarus, 181, 442
Schleicher D. G., 2010, AJ, 140, 973
Schleicher D. G., Millis R. L., Birch P. V., 1998, Icarus, 132, 397
Schulz R., Stüwe J. A., Boehnhardt H., 2004, A&A, 422, L19
Snodgrass C., Tubiana C., Bramich D. M., Meech K., Boehnhardt H., Barrera L., 2013, A&A, 557, A33
Snodgrass C. et al., 2016a, MNRAS, 462, S138
Snodgrass C. et al., 2016b, A&A, 588, A80
Snodgrass C. et al., 2017, Phil. Trans. R. Soc. A, 375, 20160249
Steele I. A. et al., 2016, MNRAS, 460, 4268
Vincent J.-B. et al., 2016, MNRAS, 462, S184

This paper has been typeset from a TEX/LATEX file prepared by the author.